INTERNATIONAL JOURNAL OF ENERGY STUDIES

e-ISSN: 2717-7513 (ONLINE); homepage: https://dergipark.org.tr/en/pub/ijes

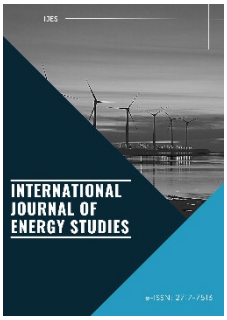


Research Article
Int J Energy Studies 2024; 9(4): 745-773
DOI: 10.58559/ijes.1412839

**Received** : 15 Jan 2024
**Revised** : 01 Sep 2024
**Accepted** : 25 Oct 2024

# Enhanced droop control for off-grid and grid-tied scenarios in renewable energy systems

**Sahin Gullu[a*], Mohammad Nilian[b], Issa Batarseh[c]**
*[a]Nevsehir Haci Bektas Veli University, Department of Electrical and Electronics Engineering, ORCID: 0000-0002-2997-172X*
*[b]University of Central Florida, Department of Electrical and Computer Engineering, ORCID: 0000-0002-0737-166X*
*[c]University of Central Florida, Department of Electrical and Computer Engineering, ORCID: 0000-0002-8420-1891*
*(*Corresponding Author: sahin.gullu@nevsehir.edu.tr)*

**Highlights**

- Grid-forming (GFM) inverters' control techniques are discussed.
- Ride-through requirements are defined to have optimum the voltage and frequency regulation control algorithm.
- The droop control method's weak points are modified to have better load sharing performance in three different Inverter Based Resources (IBRs) and the grid scenarios.

**You can cite this article as:** Gullu S, Nilian M, Batarseh I. Enhanced droop control for off-grid and grid-tied scenarios in renewable energy systems. Int J Energy Studies 2024; 9(4): 745-773.

## ABSTRACT

The control methods of Grid-forming (GFM) inverters are discussed and reviewed. Then, the droop control method's weak points are modified to have better load sharing performance and improving the lifetime of the inverters when the system has light load situations. Also, the effects of the coupling reactance on stability and reliability are investigated. This control method is applied to three different scenarios in order to see frequency and voltage stability and load sharing between three Inverter Based Resources (IBRs) and the grid. The first case is that the voltage and frequency regulation control algorithm is presented when the IBRs have equal power ratings during the off-grid. Then, the second case is also performed in islanding mode where the load sharing control algorithm is determined based on the different power ratings of the IBRs. Lastly, this setup examined the load sharing status during the grid-tied scenario when the IBRs are not capable of supplying enough power to the load. In all cases, loads are added to and removed from the system to ensure that the frequency and voltages are in the range of continuous operation.

**Keywords:** Droop control, Inverter based resources, Load sharing, Renewable energy systems

## 1. INTRODUCTION

Conventional AC power systems are dominated by synchronous generators (SG). This system has high inertia, behaves almost an ideal voltage source, and provides a stable frequency [1-3], which are essential features for maintaining a highly regulated power grid. Moreover, the current capability of SGs is typically up to six times the rated currents. Their primary objectives are voltage and frequency regulation that are achieved by exciter and governor control.

Renewable energy sources are intermittent, and they have low inertia issues. They have a low stable system. This means that solar energy systems cannot store kinetic energy in the same way that AC power systems can. As a result, they are more sensitive to sudden changes in load or generation. One of the biggest challenges posed by low inertia is the risk of cascading failures. If a large disturbance occurs, it can cause a chain reaction of outages, eventually leading to a blackout. Another challenge posed by low inertia is the risk of load shedding.

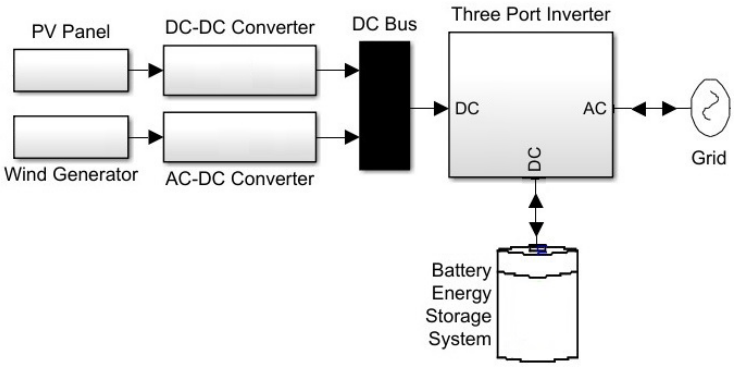


**Figure 1.** General illustration of renewable energy integration with Grid and BESS

The integration of Grid, BESS and renewable energy sources in Figure 1 can be valid in a renewable energy system. If BESS voltage is the same as DC bus voltage, it may directly be connected to the DC bus. However, it is usually an optimal decision to use high voltage BESS to decrease the current value that helps to decrease the power loss and to increase power efficiency. Also, depending on applications, the three-port inverter in Figure 1 can be replaced by a multiport or a two-port inverter; they might be unidirectional or bidirectional inverters. Multiport inverters can be single-stage inverters [4,5] or dual-stage inverters [6,7] that consist of multiple converters' integration.

When Grid is connected to the system, it is called grid-tied system; it is called off-grid system in case that Grid is not connected. Nonetheless, this entire system can be referred to as a microgrid system. Microgrids can operate in the grid-connected and in the island mode. In the grid-connected mode, voltage and frequency are regulated by the grid. Inverters follow the grid voltage and operate at grid frequency. The common technique utilized to synchronize with the grid voltage is a phase-locked loop (PLL). These inverters are current controlled inverters, and their behavior resembles a current source. Therefore, they are called grid-following (GFL) inverters. GFL inverters can be classified into two inverters. Grid-supporting inverters are usually used in large-scale inverter-based resources (IBRs) such as above 5 MW. Grid-supporting inverters supply reactive power and varying active power at predefined droop setting [2]. If the grid voltage decreases, IBRs will supply positive reactive power. If the grid voltage goes up, IBRs will supply negative reactive power. Grid-feeding inverters maintain a constant current output and provide active power in phase with the grid because they focus on MPPT and zero reactive power [2,8,9].

In contrast, in island mode, one or more inverters should function as voltage and frequency regulators to form a local grid. This particular need initiated the concept of the grid-forming (GFM) inverters. Reference [3] states that GFM was named previously "voltage forming" or "grid-voltage-forming." They can function as voltage sources. As a result of that, GFM inverters should emulate synchronous generators.

The primary objective of GFL is to deliver active power. Supporting the grid is the secondary objective. However, GFM inverters' first objective is to regulate the voltage and frequency of the grid by changing the active and reactive power references continuously. Based on the properties of synchronous generators, GFM inverters should support load sharing/drooping, black start, inertial response, and hierarchical frequency/voltage regulation [10-12].

However, there are basic challenges with GFM inverters. Firstly, the over-current ratings of the power electronic switching devices are low compared to synchronous generators. Therefore, meeting the fault current behavior of SG is challenging in GFM inverters. GFM inverters must be oversized, that makes them expensive and commercially less attractive. Secondly, the renewable energy sources have low inertia or zero inertia, so energy storage systems are required. Thirdly, they need more sophisticated control systems and demand response programs.

## 2. RIDE-THROUGH REQUIREMENTS

Ride-through is defined as the capability of an electrical system to maintain its connection in short periods when the electric network voltage or frequency becomes higher or lower. The ride-through requirements are defined by grid connection standards [13,14], which are California Rule 21 and IEEE standards 1547-2018 that are shown in Table 1 and 2.

**Table 1.** Frequency ride-through standards

| Frequency range (Hz) | Region | Disconnection time (s) |
|---|---|---|
| **61.8 < f < 66** | Over frequency II | 0.16 |
| **61.2 < f ≤ 61.8** | Over frequency I | 299 |
| **58.8 ≤ f ≤ 61.2** | Continuous operation | Infinite |
| **57 < f < 58.8** | Low frequency I | 299 |
| **50 < f ≤ 57** | Low frequency II | 0.16 |

**Table 2.** Voltage ride-through standards

| Voltage range (V) | Region | Disconnection time (s) |
|---|---|---|
| **120 < V** | Over voltage II | 0.16 |
| **110 < V ≤ 120** | Over voltage I | 12 |
| **88 ≤ V ≤ 110** | Continuous operation | Infinite |
| **70 ≤ V < 88** | Low voltage I | 20 |
| **50 ≤ V < 70** | Low voltage II | 10 |
| **V < 50** | Low voltage III | 1 |

For the frequency requirements, both GFL and GFM inverters must be disconnected from the grid immediately if the frequency exceeds 66 Hz or goes down below 50 Hz. When the frequency is in over frequency region II (61.8 Hz to 66 Hz) and low frequency region II (50 Hz to 57 Hz), the circuit breaker should trip in 0.16 seconds. During over frequency region I (61.2 Hz to 61.8 Hz) and low frequency region II (57 Hz to 58.8 Hz), the inverters can keep their connections to grid for up to 299 seconds.

For the over voltage region II, the inverters must be disconnected from the grid in 0.16 seconds when the voltage exceeds 120 V. If the voltage value is between 110 V to 120 V, the connection should be tripped in 12 seconds. For the low voltage regions, there are three regions. The inverters

can remain connected for up to 20 seconds, 10 seconds and 1 second if the voltage levels are between 70 V to 88 V, 50 V to 70 V, and below 50 V, respectively.

These requirements originated from grid-connected GFL inverters. The implementation of these requirements for GFM inverters is also valid in the grid connected mode and islanding mode for further modification in the standards [11].

## 3. CONTROL TECHNIQUES

Voltage regulation becomes challenging at the point of common coupling (PCC) in weak grids. A weak grid is an electrical power system that is unable to provide reliable and stable power supply due to its limited capacity and voltage regulation capabilities. It is typically characterized by a low capacity to generate, transmit, and distribute electrical power. An MPPT algorithm is sent to the grid "Grid-support function," then it generates modified $P^*$ and $Q^*$. A current algorithm generates direct and quadrature line currents magnitude and phase angle to achieve the active and reactive power outputs. The frequency is the same as the grid frequency. The most critical status is grid synchronization to deliver power in GFL inverters, which is usually done by PLL algorithm. After grid synchronization, control references are sent to each control block to achieve the desired performance [11].

In contrast GFL inverters, GFM inverters do not measure the voltage at PCC for phase angle and frequency purposes, it forms the voltage. In normal grid-connected operations, the GFM inverter follows the power references from a system-level controller or an MPPT algorithm to generate high-quality power as GFL inverters do. However, under abnormal grid conditions or islanding conditions, the GFM inverter is capable of sustaining its own voltage and frequency based on preset references without the PLL unit.

The control methods for GFM inverters can be classified as shown below. The droop control method and the simulation scenarios are discussed thoroughly in the next section. However, in this section, the literature review of five control techniques is explained.

1) Droop control.
2) Swing equation emulation control.
3) Power synchronization control.

4) Virtual synchronization machine control.
5) Virtual oscillator-based control.
6) Augmented virtual synchronization generator control.
7) Synchronverter control.
8) Matching control.
9) H2/Hꝏ based robust structure control.
10) Frequency shaping based control.

### 3.1. Droop Control

Even though Droop control is a control method commonly used in grid-forming inverters to regulate the output power and frequency of the inverter and maintain synchronization with the grid [15-17], it is typically used in systems where multiple inverters are connected to the grid in parallel [2]. The basic idea behind droop control is to use a droop function to regulate the output power and frequency of the inverter based on the difference between the inverter's output frequency and the grid frequency. The droop function is a linear or non-linear function that relates the inverter's output frequency to its active output power, and the inverter's output voltage to its reactive output power. One of the key advantages of droop control is its simplicity and scalability. It allows for many inverters to be connected to the grid in parallel, while ensuring that they operate in a stable and synchronized manner. It also allows for easy integration of renewable energy sources, such as solar or wind power, into the grid. Even though the first use of such controllers is in isolated AC power systems and uninterruptible power supplies (UPS), they can be utilized for operating large, interconnected power grids.

In droop control, the frequency (ω) of the inverter is allowed to decrease linearly with the increasing the active power (P) in the active power controller (APC). Droop control mechanism can be utilized in the reactive power controller (RPC) to control the voltage magnitude based on reactive power (Q). Similar to the APC, the voltage magnitude at the PCC is linearly drooped based on the reactive power injection of the inverter. This linear P-ω drooping behavior is defined using a droop coefficient. The transfer function for the droop control ($K_{droop}$) is as follows:

$$K_{droop} = \frac{\Delta\omega}{\Delta P} = K_{P\rightarrow\omega} \quad (1)$$

where $K_{P\rightarrow\omega}$ is the droop coefficient. The droop coefficient is chosen in the standalone mode such that the load is shared based on the power ratings of the inverters. The droop controller is usually used with a low-pass filter to filter out high frequency harmonics.

### 3.2. Swing Equation Emulation Control

Swing equation emulation control is a control method that is used in grid-forming inverters to emulate the behavior of a synchronous generator [2,17]. It is based on the mathematical model of the swing equation that describes the dynamics of a synchronous generator and relates the generator's mechanical power output to its rotor angle and frequency. The swing equation emulation control algorithm operates by monitoring the power flow between the inverter and the grid and adjusting the inverter's output voltage and frequency based on the swing equation model. One of the key advantages of swing equation emulation control is that it enables grid-forming inverters to provide the same level of stability and reliability as synchronous generators, while also offering the flexibility and efficiency benefits of inverters.

The swing equation of a synchronous generator as:

$$P_d = D_d(\omega - \omega_g) \quad (2)$$

$$M\frac{d(\omega - \omega_g)}{dt} + D_d(\omega - \omega_g) = P_m - P_e \quad (3)$$

where $\omega_g$, $\omega$, $D_d$, M, $P_m$, $P_e$, and $P_d$ are grid frequency, output frequency, damping coefficient, inertia coefficient, mechanical power, electrical power, and damping power, respectively.

### 3.3. Power Synchronization Control

In a GFM inverter, power synchronization control (PSC) is a method used to synchronize the inverter's output power with the power grid. This is necessary to ensure that the inverter can supply power to the grid in a stable and reliable manner, and to prevent any disruptions or damage to the grid. One of the key challenges in power synchronization control is ensuring that the inverter's output voltage and frequency are in phase with the grid voltage and frequency. This requires

precise control of the inverter's output waveform, and the ability to quickly respond to changes in the grid conditions. To achieve this level of control, power synchronization control algorithms typically use advanced control techniques, such as proportional-integral-derivative (PID) control or model predictive control (MPC).

In PSC, the synchronization with the grid is achieved similar to a synchronous machine through transient power transfer. In the PSC, instead of the frequency, the phase angle is droop based on the power increment. The transfer function of the PSC controller (KPSC):

$$K_{PSC} = \frac{\Delta\theta}{\Delta P} = \frac{K_{P\rightarrow\theta}}{s} \tag{4}$$

where $K_{P\rightarrow\theta}$ is the controller gain. Typically, in PSC, a DC-link voltage controller cascades with the active power loop. The gain for the active power loop is chosen based on an open-loop transfer function that includes the effect of active resistance. The robustness is guaranteed by ensuring stability margins for phase ($\phi_m$) and gain ($g_m$) margins of the open-loop transfer function are within the recommended ranges ($\phi_m \geq 45^0$, $g_m \geq 2$).

### 3.4. Virtual Synchronization Machine Control

Virtual synchronization machine (VSM) control is a control method used in GFM inverters to simulate the behavior of a synchronous generator and maintain synchronization with the power grid. It is desirable to have GFM inverters that can provide the same level of stability and reliability. The VSM control algorithm operates by emulating the behavior of a synchronous generator's mathematical model and using this model to adjust the inverter's output voltage and frequency to match the grid conditions.

The VSM model is based on a complete two-shaft synchronous machine model that includes stator windings, damper windings, and excitation windings, which are modeled in a process computer [12]. The machine currents are calculated in real-time based on the measured voltage at the PCC and fed into the grid. The active power and reactive power are controlled based on the virtual torque and virtual excitation voltage, respectively.

### 3.5. Virtual Oscillator-based Control

Virtual oscillator-based control is a control method used in power electronics systems to simulate the behavior of an oscillator and regulate the output voltage and frequency of the system. It is commonly used in grid-tied inverters. The basic idea behind virtual oscillator-based control is to use a mathematical model of an oscillator to regulate the output voltage and frequency of the inverter.

The oscillator model is designed to mimic the behavior of a physical oscillator, which generates a sinusoidal waveform with a specific frequency and phase. By simulating the behavior of an oscillator, the inverter can generate its own reference signal and operate in synchronization with other inverters in the system.

## 4. IMPROVED DROOP CONTROL METHODOLOGY

Power flow theory in Figure 2 is used to explain which parameters affect the active and reactive power. Then, the frequency and voltage changes are defined depending on whether it is a transmission line or a distribution line [18].

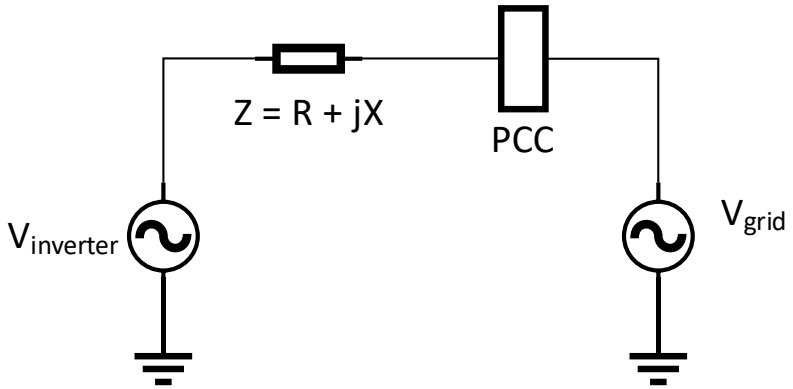


**Figure 2.** General illustration of power flow in a line

### 4.1. Theory

The power flow in a line is explained theoretically in Equation (5) through Equation (13).

$$S = V_1 \cdot I^* = V_1 \cdot \left(\frac{V_1 - V_2}{Z}\right)^* \quad (5)$$

$$P + jQ = \frac{V_1^2}{Z} e^{j\theta} - \frac{V_1 \cdot V_2}{Z} e^{j(\theta+\delta)} \quad (6)$$

$$P = \frac{V_1^2}{Z} cos(\theta) - \frac{V_1 \cdot V_2}{Z} cos(\theta + \delta) \quad (7)$$

$$Q = \frac{V_1^2}{Z} sin(\theta) - \frac{V_1 \cdot V_2}{Z} sin(\theta + \delta) \quad (8)$$

$$Z = R + jX \quad (9)$$

$$P = \frac{V_1^2}{\sqrt{R^2 + X^2}} \cdot \frac{R}{\sqrt{R^2 + X^2}} - \frac{V_1 \cdot V_2}{\sqrt{R^2 + X^2}} \cdot \left( \frac{R}{\sqrt{R^2 + X^2}} cos\, \delta - \frac{X}{\sqrt{R^2 + X^2}} sin\, \delta \right) \quad (10)$$

$$P = \frac{V_1}{(R^2 + X^2)} \cdot [R \cdot (V_1 - V_2\, cos\, \delta) + V_2 \cdot X \cdot sin\, \delta] \quad (11)$$

$$Q = \frac{V_1^2}{\sqrt{R^2 + X^2}} \cdot \frac{X}{\sqrt{R^2 + X^2}} - \frac{V_1 \cdot V_2}{\sqrt{R^2 + X^2}} \cdot \left( \frac{X}{\sqrt{R^2 + X^2}} cos\, \delta + \frac{R}{\sqrt{R^2 + X^2}} sin\, \delta \right) \quad (12)$$

$$Q = \frac{V_1}{(R^2 + X^2)} \cdot [X \cdot (V_1 - V_2\, cos\, \delta) - V_2 \cdot R \cdot sin\, \delta] \quad (13)$$

In case of a transmission line, $X \gg R$ and $\delta\ is\ small$, so that $R \approx 0$, $\sin \delta \approx \delta, and\ cos\, \delta \approx 1$. The power angle depends on the active power and the voltage change depends on the reactive power as shown in Equation (14), (15), (16) , (17) and (18).

$$P = \frac{V_1 \cdot V_2 \cdot \delta}{X} \quad (14)$$

$$\delta = \frac{P \cdot X}{V_1 \cdot V_2} \quad (15)$$

$$\delta = \int (\omega - \omega_0)\, dt \quad (16)$$

$$Q = \frac{V_1 \cdot (V_1 - V_2)}{X} \tag{17}$$

$$(V_1 - V_2) = \frac{Q \cdot X}{V_1} \tag{18}$$

Figure 3 shows the droop control characteristic of active and reactive power that affects the frequency and voltage stability. The amount of the active droop coefficients ($m_p$) is determined by the maximum frequency change and maximum active power change whereas the amount of the reactive droop coefficients ($m_q$) is determined by the maximum voltage change and maximum reactive power change, which are expressed in Equation (19) and (20).

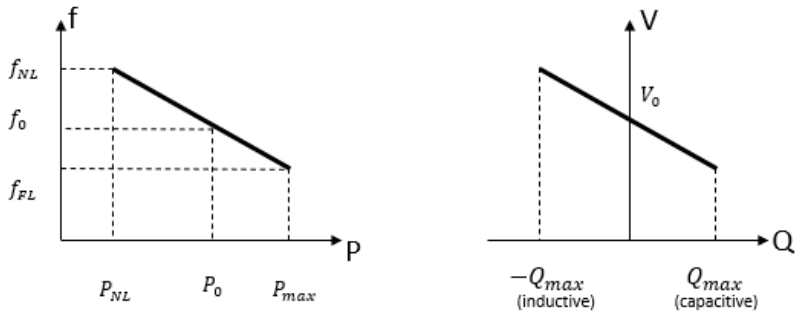


**Figure 3.** Droop control (negative feedback control) for frequency and voltage.

$$(f - f_0) = -m_p(P - P_0) \tag{19}$$

$$(V - V_0) = -m_q(Q - Q_0) \tag{20}$$

where f is measured frequency, $f_0$ is desired frequency, $m_p$ and $m_q$ are droop coefficients, $P$ is measured active power, $P_0$ is rated power, $Q$ is rated reactive power, $Q_0$ is measured reactive power. However, for microgrid applications or distribution lines, R cannot be ignored. Therefore, when both R and X are considered, the voltage and frequency are dependent on both reactive and active power as derived in Equation (21) and (22).

$$(f - f_0) = -m_p(P - P_0)\frac{X}{Z} + m_q(Q - Q_0)\frac{R}{Z} \tag{21}$$

$$(V - V_0) = -m_p(P - P_0)\frac{R}{Z} - m_q(Q - Q_0)\frac{X}{Z} \quad (22)$$

### 4.2. Control Algorithm Block Diagrams

As shown in Figure 4, there are five main blocks in order to control the voltage and frequency of the system. First of all, the voltage and current are measured at the inverters' end. These measured values are sent to the DQ transformation because PID controller can be applied only DC values. Therefore, AC values from voltage and current are transformed to DQ values. Then, the active and reactive powers are calculated. After that, in order to reduce the noise and high frequency harmonics, the calculated powers are sent to a low pass filter. After the low pass filter, those values go through the frequency and voltage droop control blocks to have the reference voltage and angle. Lastly, the reference voltage, the angle, and the inverters' DQ values are sent to the PI controller in order to obtain PWM signals that are fed to the inverters.

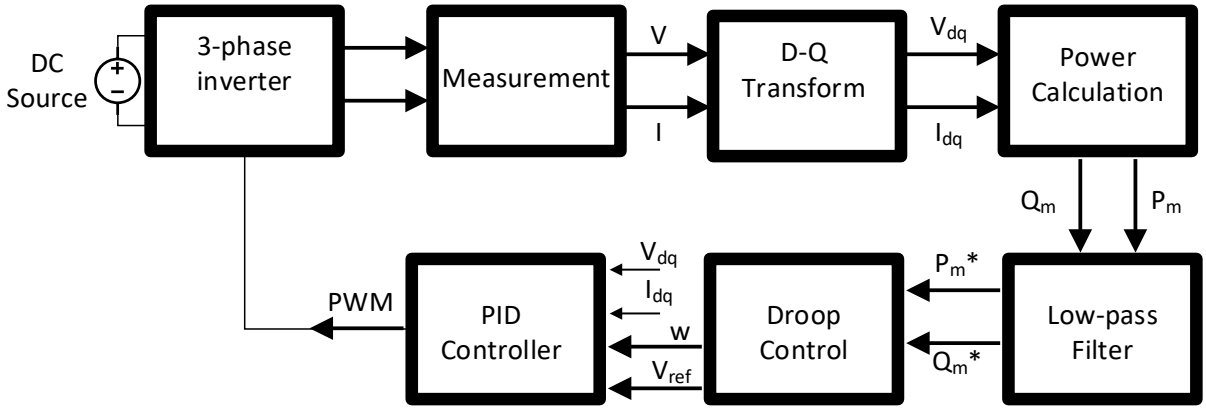


**Figure 4.** Block diagram of droop control algorithm

Equations (23) and (24) are utilized for finding the measured active and reactive power from DQ values as shown in Figure 5 and Figure 6.

$$P_m = \frac{3}{2}(V_d \cdot I_d + V_q \cdot I_q) \quad (23)$$

$$Q_m = \frac{3}{2}(V_q \cdot I_d - V_d \cdot I_q) \quad (24)$$

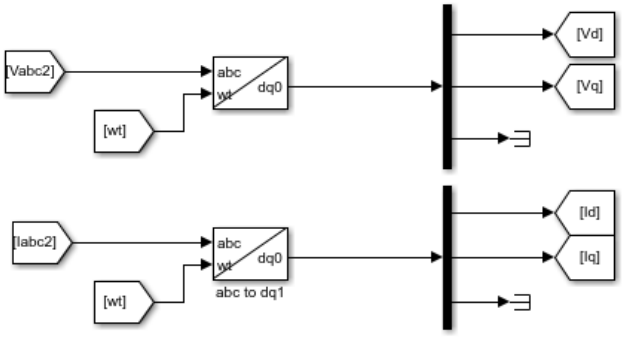


**Figure 5.** DQ transformation

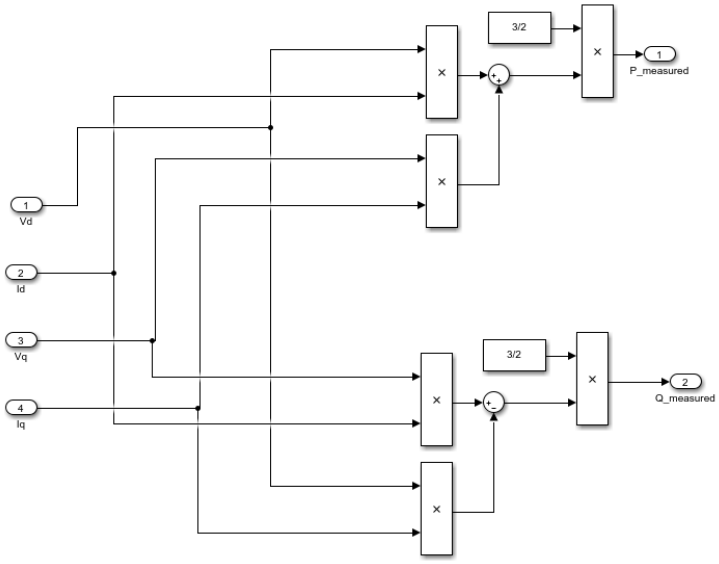


**Figure 6.** Active and reactive power calculation

Then, these measured power values are sent to a low pass filter as seen Equations (25) and (26).

$$P_m^* = \frac{w_c}{s + w_c} P_m \tag{25}$$

$$Q_m^* = \frac{w_c}{s + w_c} Q_m \tag{26}$$

After that, the modified power values go through the droop control to find the angle and the reference voltage as shown in Figure 7, Equations (27) and (28).

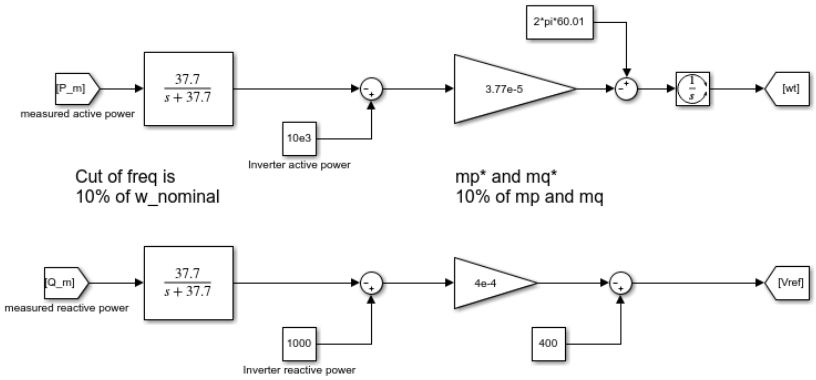


**Figure 7.** Low pass filter and droop control parameters

$$w^* = w_{NL} - m_p(P_{inverter} - P_m^*) \tag{27}$$

$$V^* = V_{NL} - m_q(Q_{inverter} - Q_m^*) \tag{28}$$

In order to obtain the frequency and voltage droop coefficients, Equations (29) and (30) are calculated.

$$m_p = \frac{\Delta w}{\Delta P_{inverter\_max}} \tag{29}$$

$$m_q = \frac{\Delta V}{\Delta Q_{inverter\_max}} \tag{30}$$

After calculating values from Equations (23) through (30), those values are sent to the PI controller in order to generate PWM signals for the GFM inverters as explicitly shown in Figure 8.

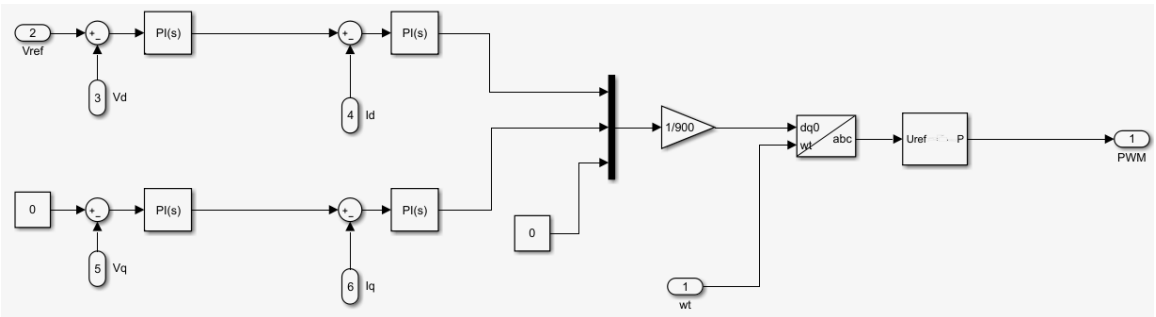


**Figure 8.** PWM generation using PI controllers

Even though Reference [19], [20], [21], and [22] claim Equation (31) and (32) to have load sharing between inverters, applying only these equations does not satisfy the load sharing due to the nature of droop control. Also, in those papers' simulation and experiments, the results show only active power sharing. Reactive power sharing cannot be achieved by simply applying the load sharing equations unless a modification in the filters of the inverters and PI controller tuning are taken into consideration.

$$m_{p1} \cdot P_{inverter\_1} = m_{p2} \cdot P_{inverter\_2} \tag{31}$$

$$m_{q1} \cdot Q_{inverter\_1} = m_{q2} \cdot Q_{inverter\_2} \tag{32}$$

### 4.3. Effect of Coupling Reactance

If a GFM inverter's coupling reactance ($X_{L2}$) in Figure 9 is too small, then this leads the system into instability [23]. Therefore, the coupling reactance value is increased until the system reaches stability. Reference [23] discusses the small signal stability boundary by observing the relationship between the PI controller parameter ($k_p$) and the coupling reactance ($X_{L2}$). That boundary condition was found from simulation results.

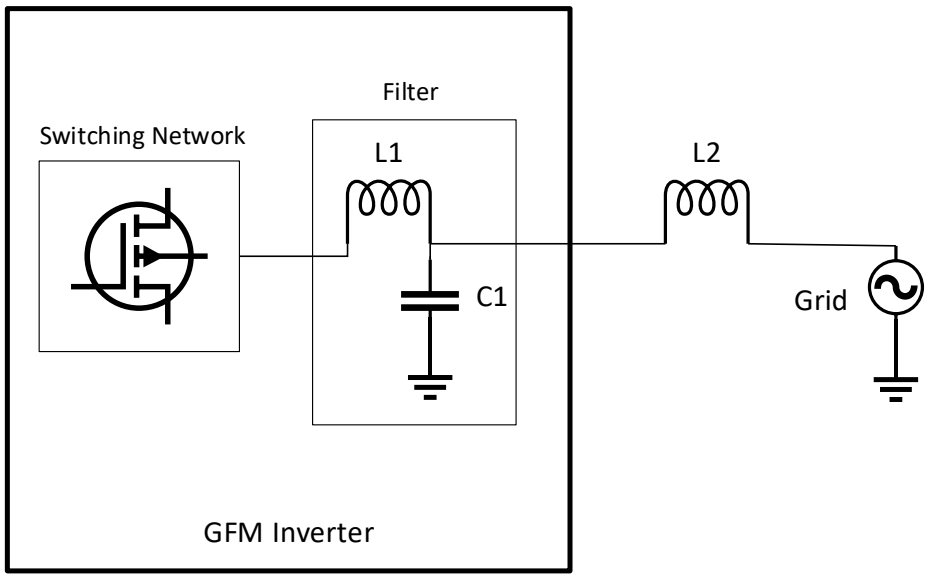


**Figure 9.** Illustration of LCL filter in a GFM inverter

## 5. RESULTS

The first scenario is to observe the frequency and voltage values in three IBRs that have equal power ratings, 10 KVA, as the simulation setup is shown in Table 3 and Figure 10.

**Table 3.** The first scenario's values

| Item | Value |
|---|---|
| Input voltage | 900 VDC |
| Switching frequency | 20 kHz |
| Inverter Powers | 10 KVA |
| Output Voltage | 400 VAC |
| L1 | 16 mH |
| C1 | 100 uF |
| L2 | 10 mH |
| Load 1 | 22 KVA |
| Load 2 | 3 KVA |

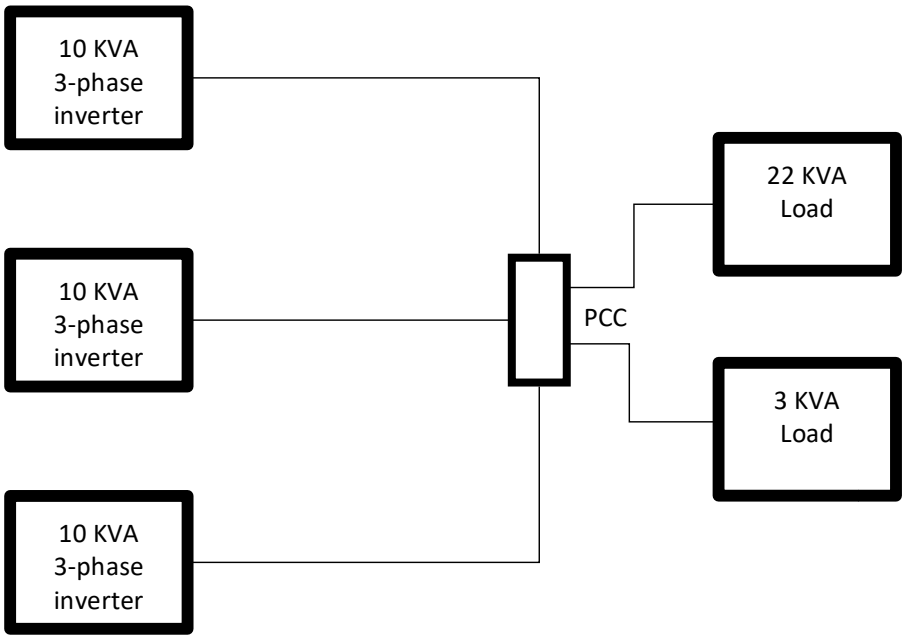


**Figure 10.** Equal IBRs scenario's setup

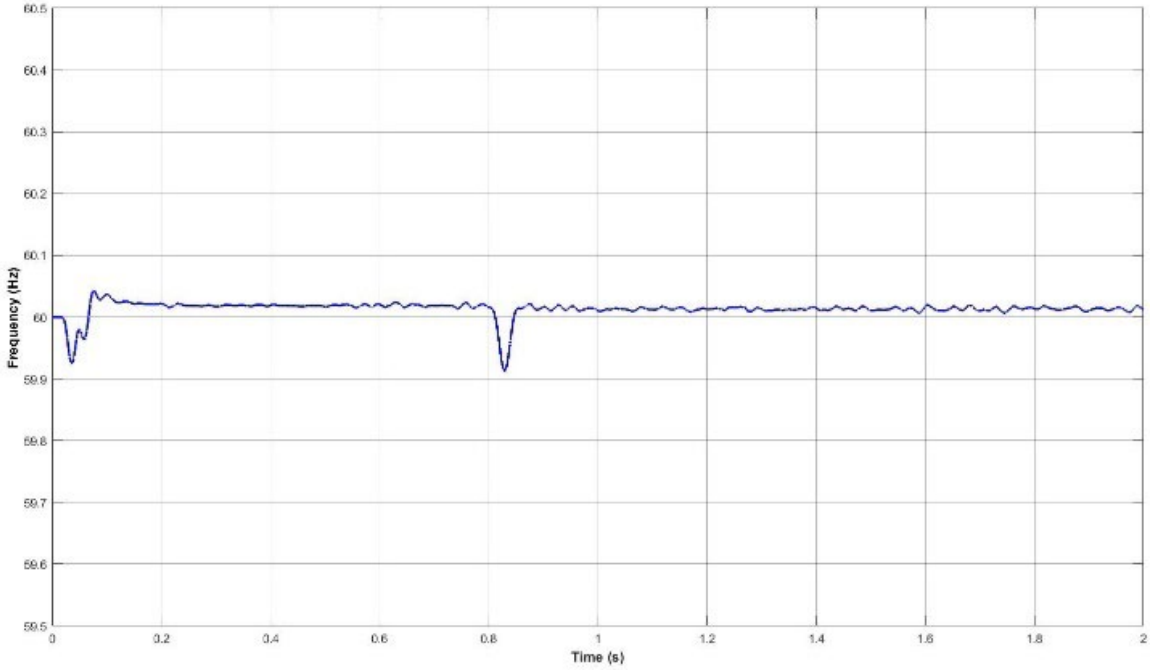


**Figure 11.** Frequency waveform for equal IBRs scenario

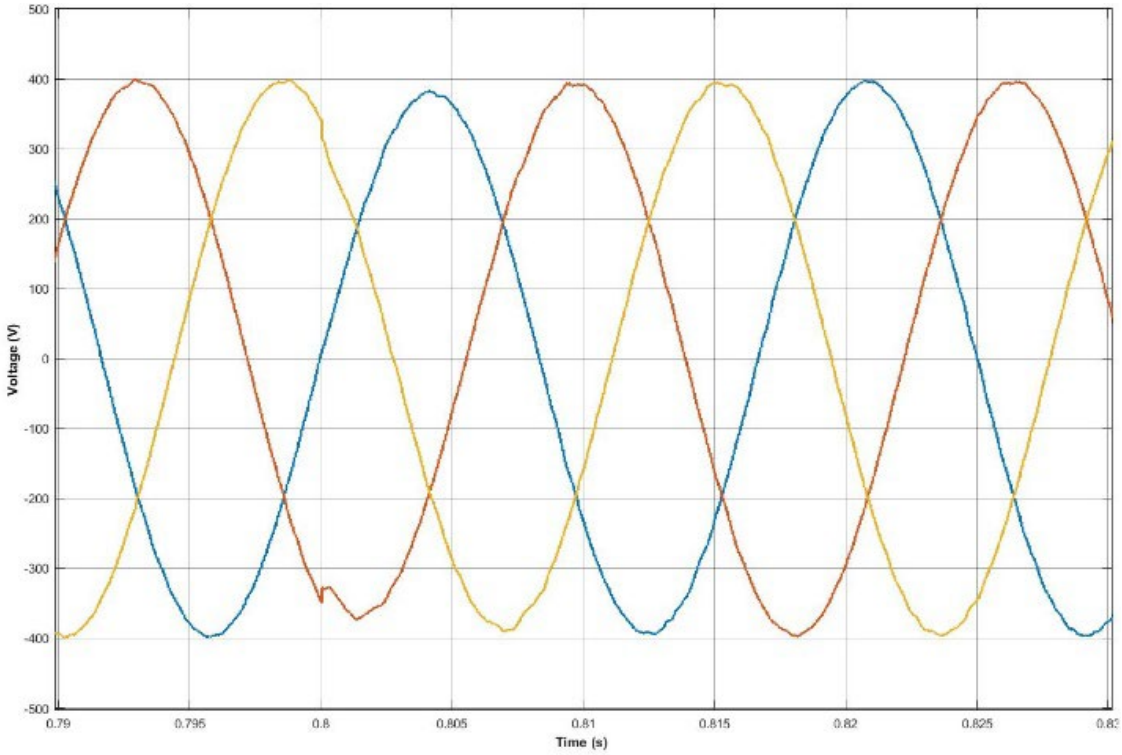


**Figure 12.** Voltage waveform for equal IBRs scenario

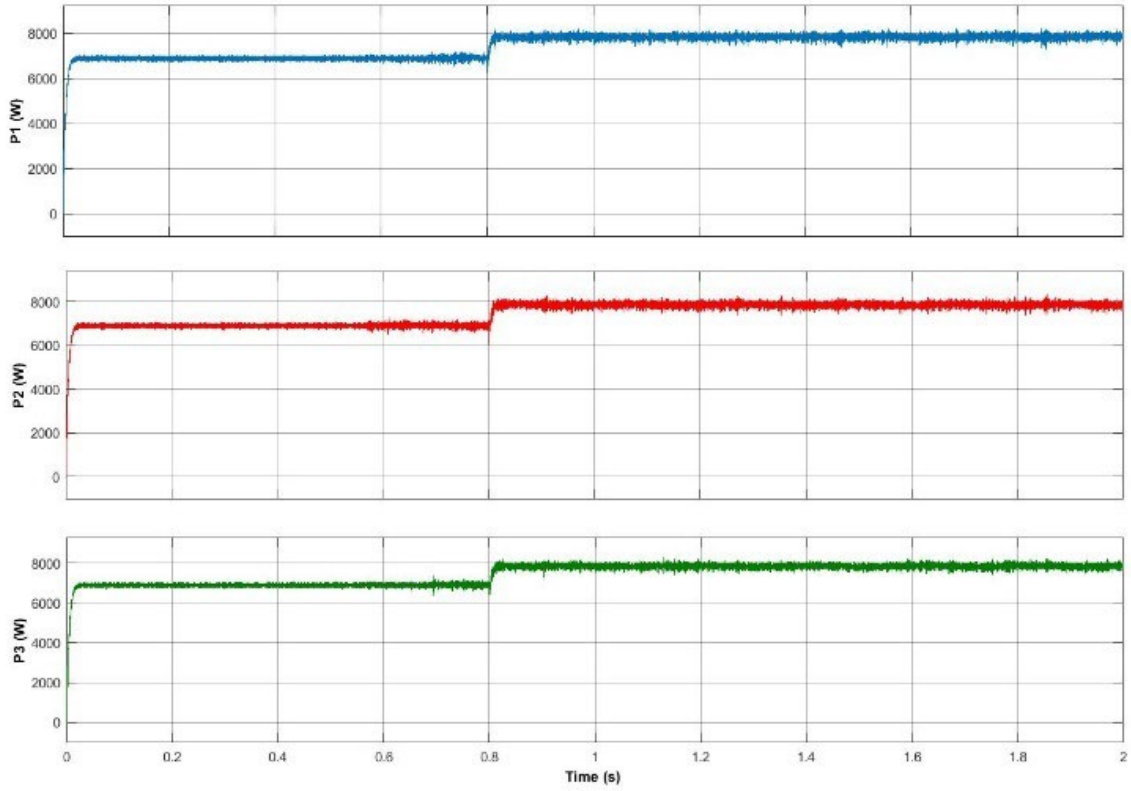


**Figure 13.** Active power for equal IBRs scenario

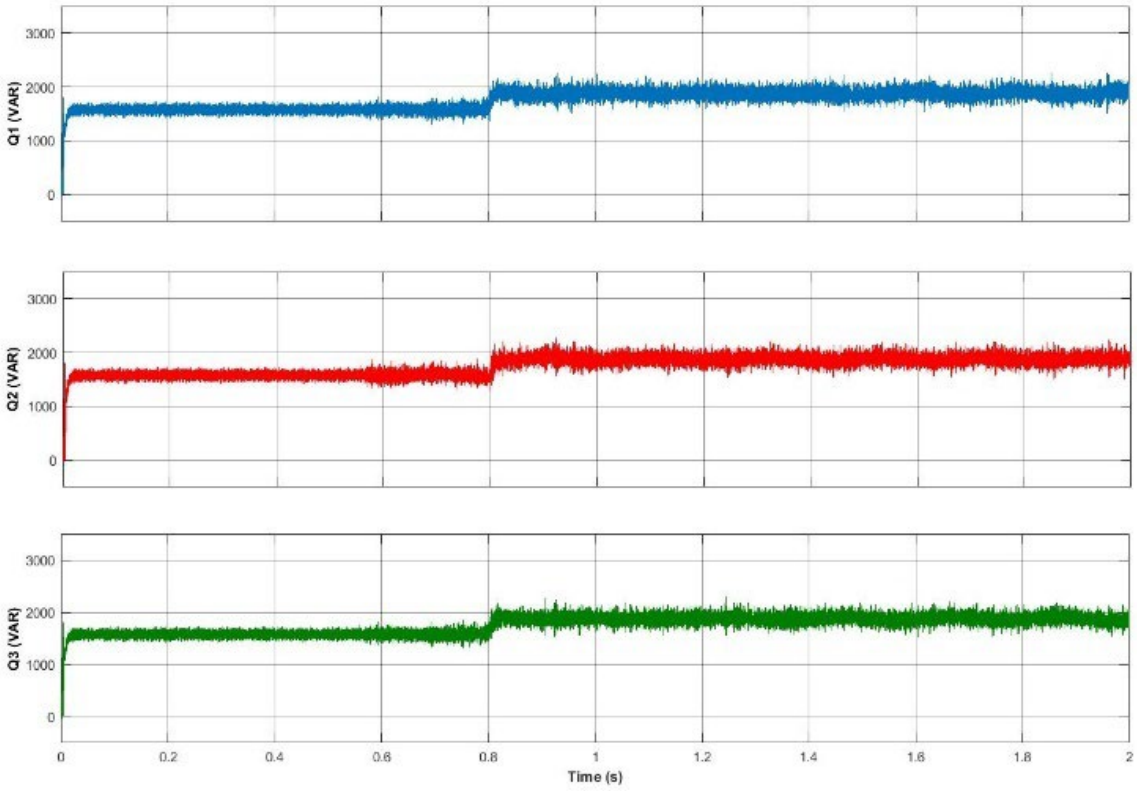


**Figure 14.** Reactive power for equal IBRs scenario

As seen in Figures 11, 12, 13 and 14, there is a change at 0.8 s because a new load, 3 KVA, is added to the system. It can be also seen that load sharing between IBRs are equal when the active power and reactive power plots are observed due to the fact that the IBRs have equal power ratings. The frequency and voltage are kept in desired values, 60 Hz and 400 V. Even after the change is applied, the frequency and voltage are recovered quickly.

The second scenario in Table 4 and Figure 15 is for different power ratings IBRs. Also, when a new load is added to the system at 2 s, the changes in frequency and voltage are less than 0.1 percent as plotted in Figure 16 and 17. Moreover, the IBRs provide power to the load based on their power ratings in Figure 18 and 19 meaning that the higher IBR supplies higher power.

**Table 4.** The second scenario's values

| **Item** | **Value** |
|---|---|
| Input voltage | 900 VDC |
| Switching frequency | 20 kHz |
| First Inverter Power | 25 KVA |
| Second Inverter Power | 12 KVA |
| Third Inverter Power | 10 KVA |
| Output Voltage | 400 VAC |
| L1-1 | 16 mH |
| C1-1 | 100 uF |
| L1-2 | 3.2 mH |
| L2-1 | 16 mH |
| C2-1 | 100 uF |
| L2-2 | 7 mH |
| L3-1 | 16 mH |
| C3-1 | 100 uF |
| L3-2 | 10 mH |
| Load 1 | 36 KVA |
| Load 2 | 3.6 KVA |

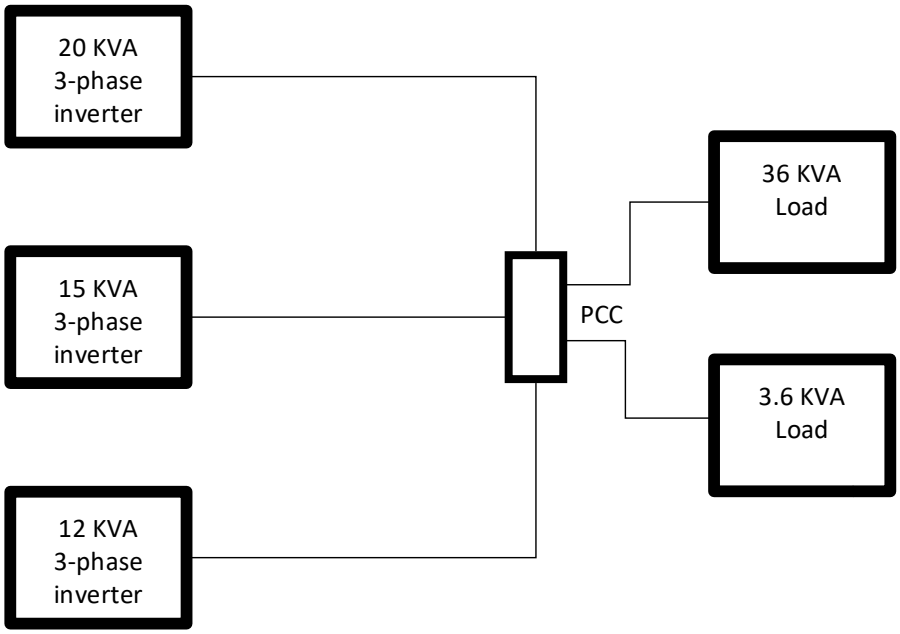


**Figure 15.** Different IBRs scenario's setup

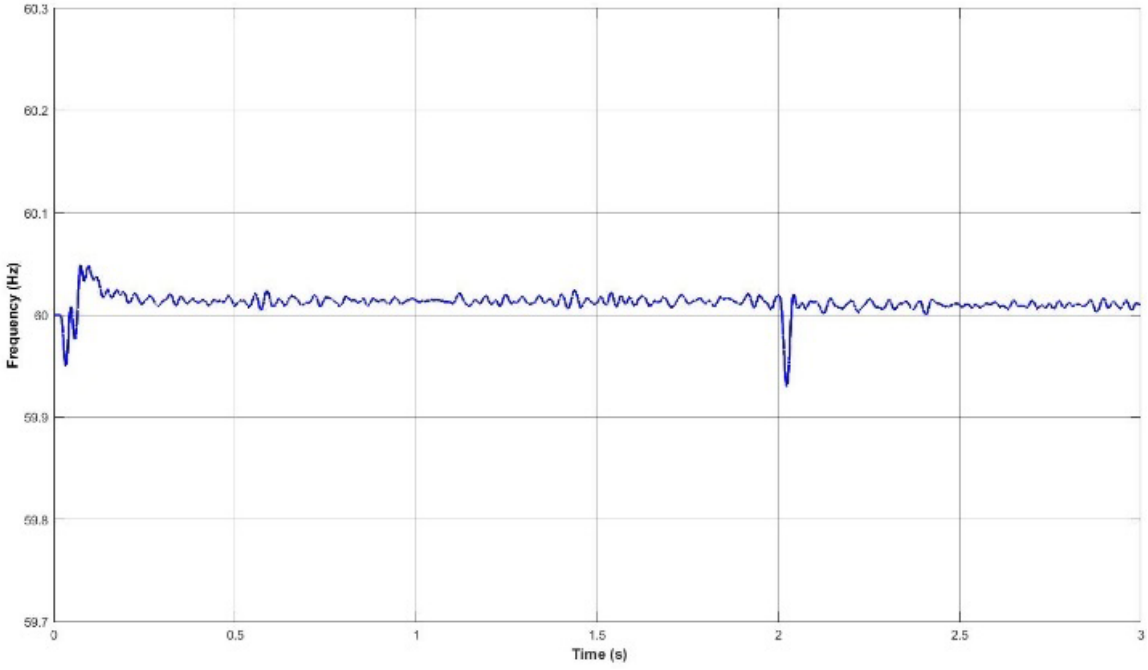


**Figure 16.** Frequency waveform for different IBRs scenario

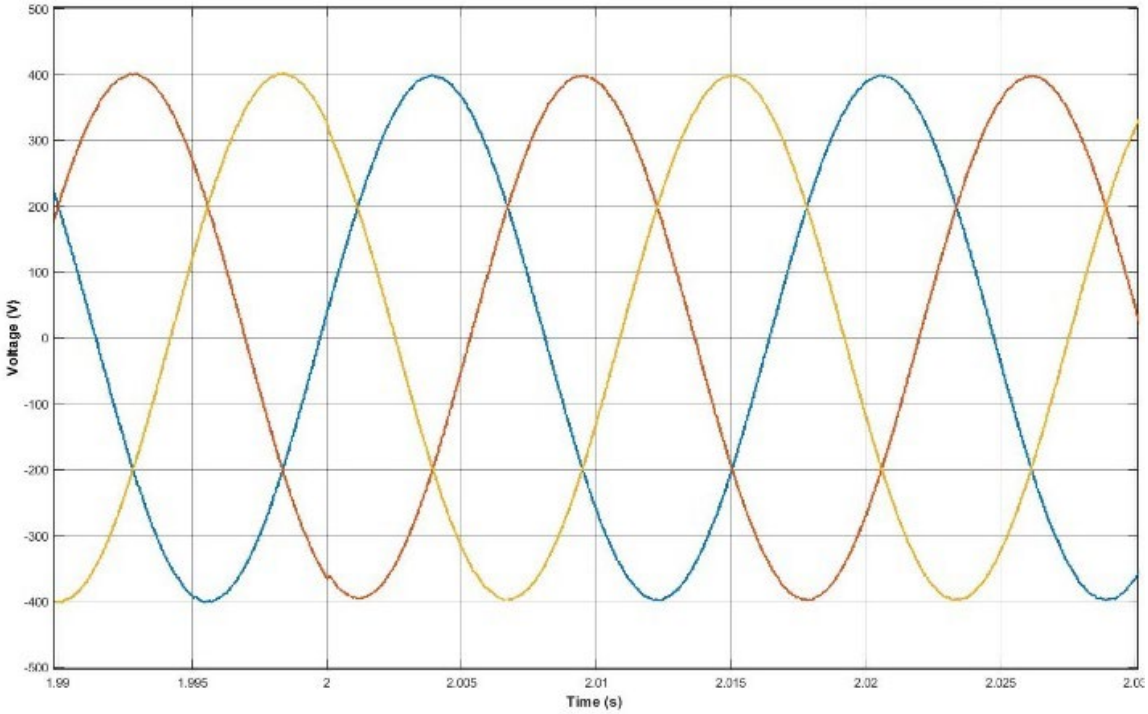


**Figure 17.** Voltage waveform for different IBRs scenario

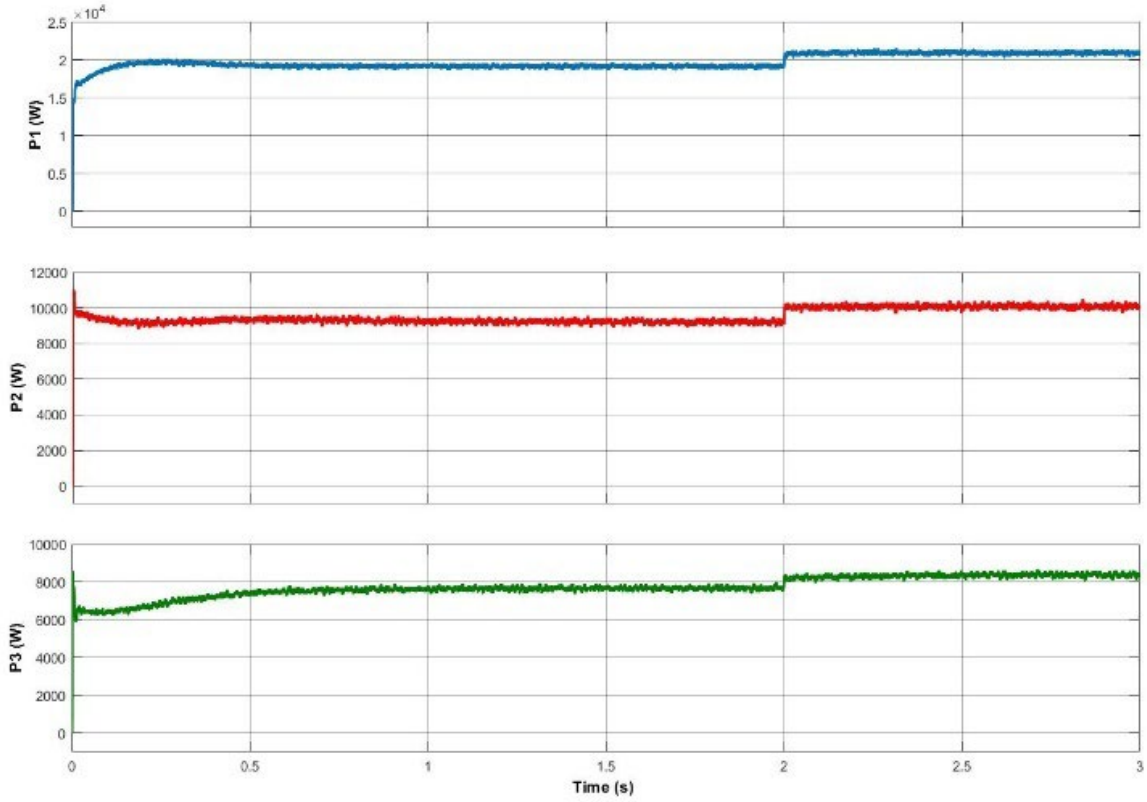


**Figure 18.** Active power for different IBRs scenario

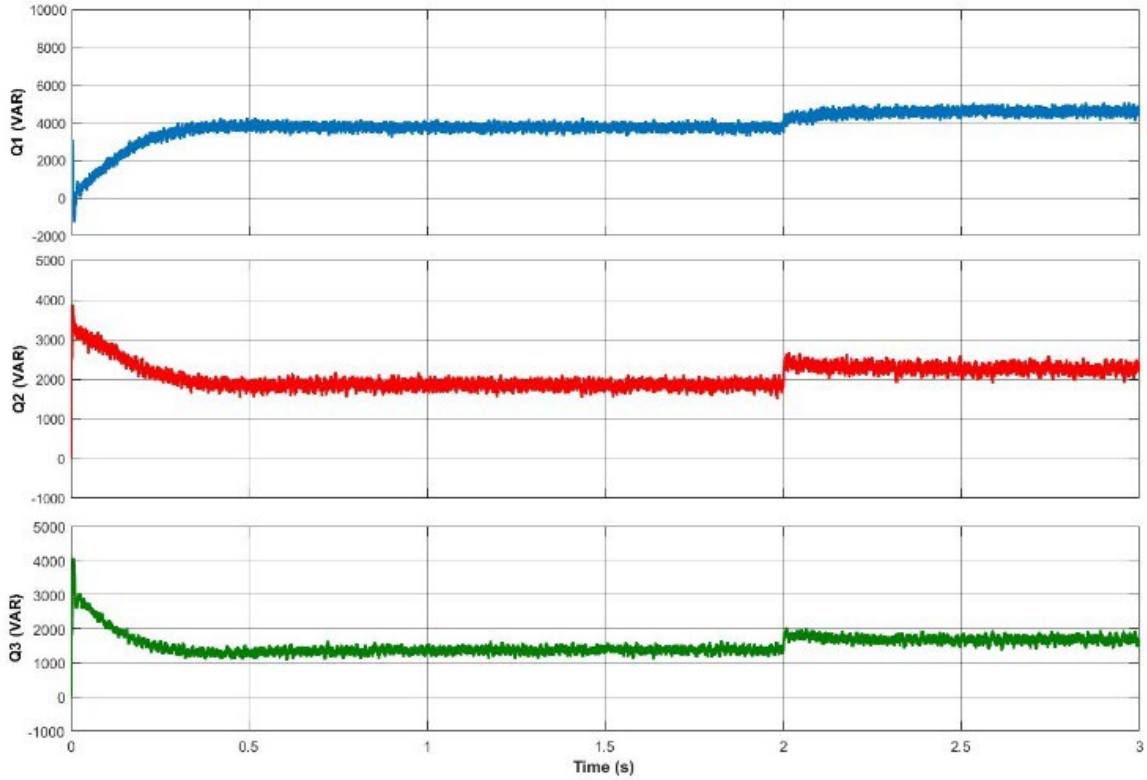


**Figure 19.** Reactive power for different IBRs scenario

The third scenario is the grid-tied scenario with three different power ratings IBRs as shown in Table 5 and in Figure 20. When the simulation starts, the total load is 39 KVA. Then, 12 KVA load is added to the system at 1 second. The fluctuation in frequency and voltage can be observed in Figure 21 and 22. It is noticed that when the grid is connected, the voltage and frequency are cleaner because the IBRs follow the grid's frequency and voltage. When a new load is added, the total load power exceeds the total IBRs power. Then, the grid is connected; the power needed for the load is taken from the grid. When 9 KVA load is removed from the system for 3 seconds, the total load power becomes less than the IBRs power. Then, the switch at the grid connection is turned off, the power from the grid becomes zero as simulated in Figure 23 and 24. After that, 30 KVA load is also removed from the system at 4 seconds, the total load becomes 12 KVA. Therefore, the 12 KVA inverter can supply the necessary power for the load, all the inverters and the grid powers are zero except the powers of the second inverter.

**Table 5.** The third scenario's values

| Item | Value |
|---|---|
| Input voltage | 900 VDC |
| Switching frequency | 20 kHz |
| First Inverter Power | 25 KVA |
| Second Inverter Power | 12 KVA |
| Third Inverter Power | 10 KVA |
| Output Voltage | 400 VAC |
| L1-1 | 16 mH |
| C1-1 | 100 uF |
| L1-2 | 3.2 mH |
| L2-1 | 16 mH |
| C2-1 | 100 uF |
| L2-2 | 7 mH |
| L3-1 | 16 mH |
| C3-1 | 100 uF |
| L3-2 | 10 mH |
| Load 1 | 30 KVA |
| Load 2 | 9 KVA |
| Load 3 | 12 KVA |

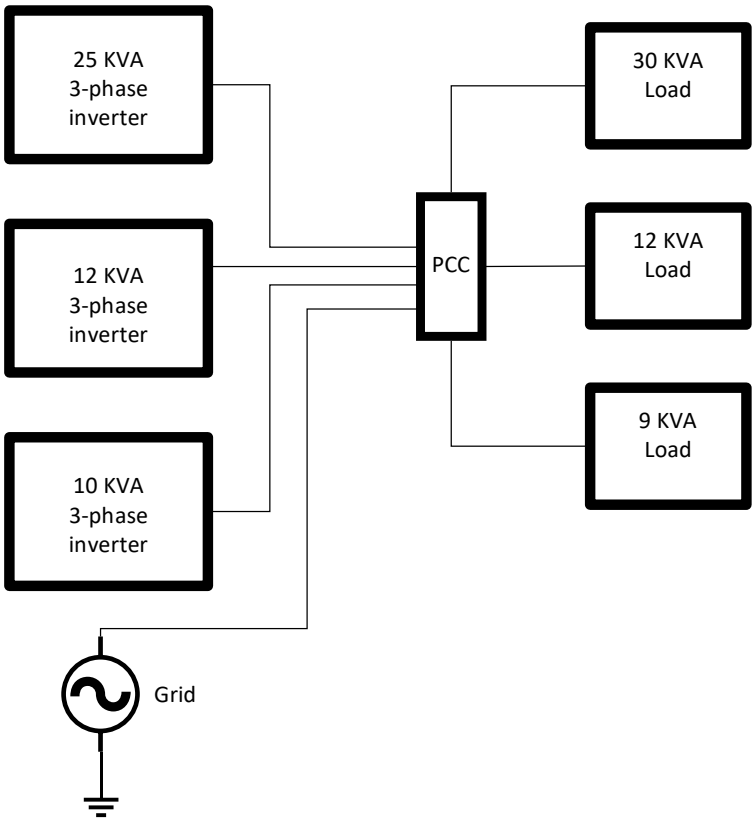


**Figure 20.** Grid-connected and IBRs scenario's setup

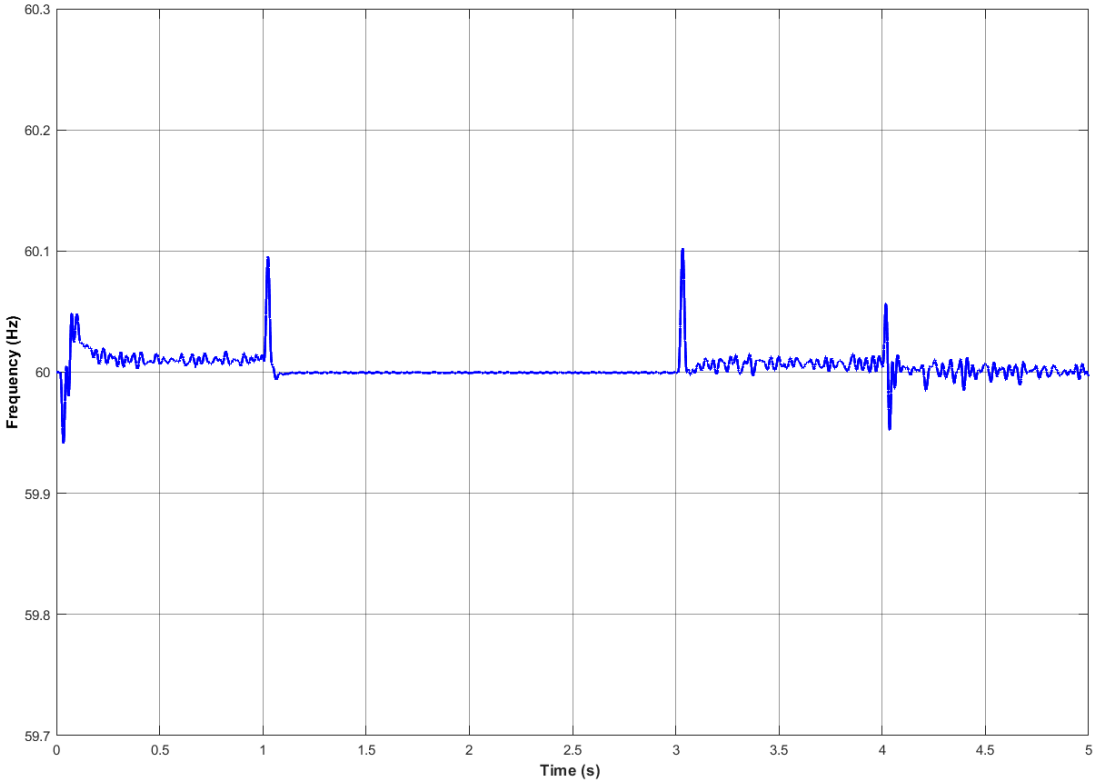


**Figure 21.** Frequency waveform for grid-tied scenario

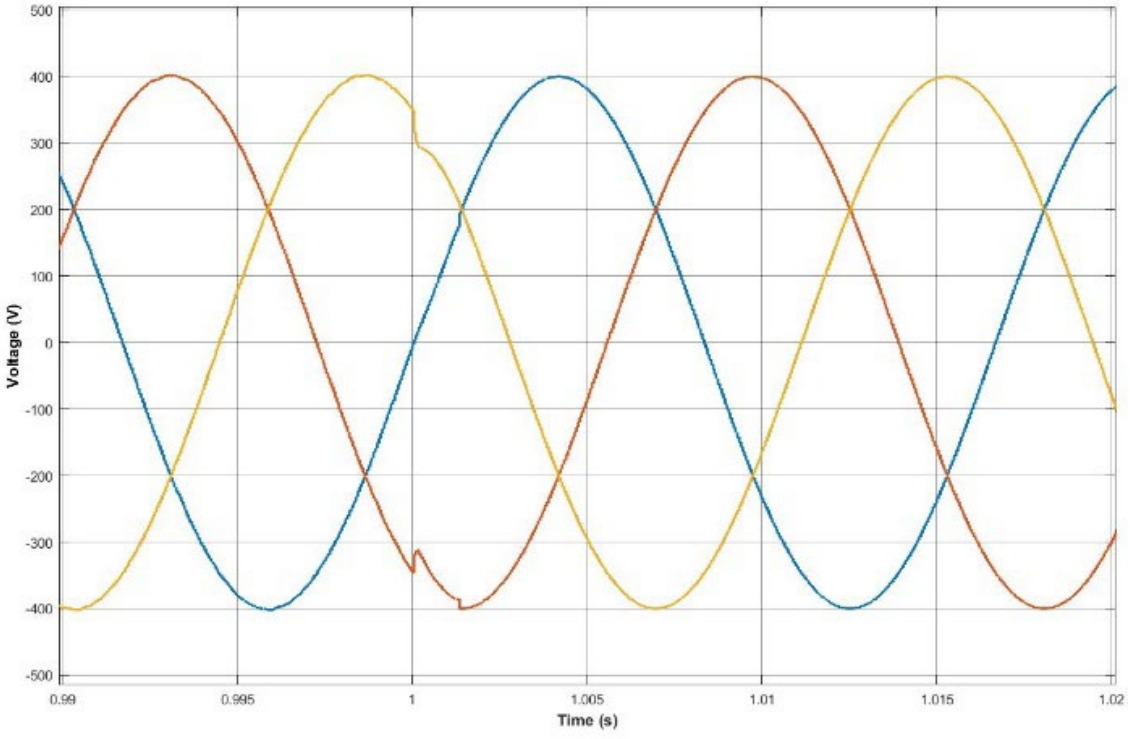


**Figure 22.** Voltage waveform for grid-tied scenario

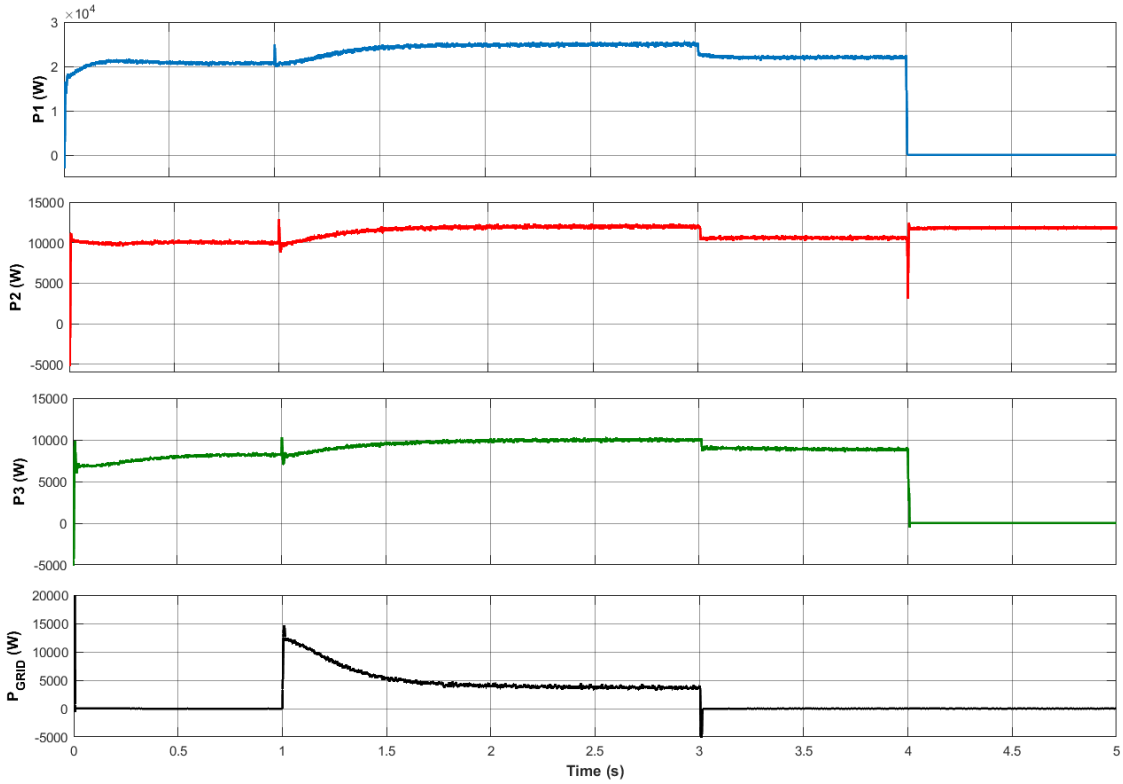


**Figure 23.** Active power for grid-tied scenario

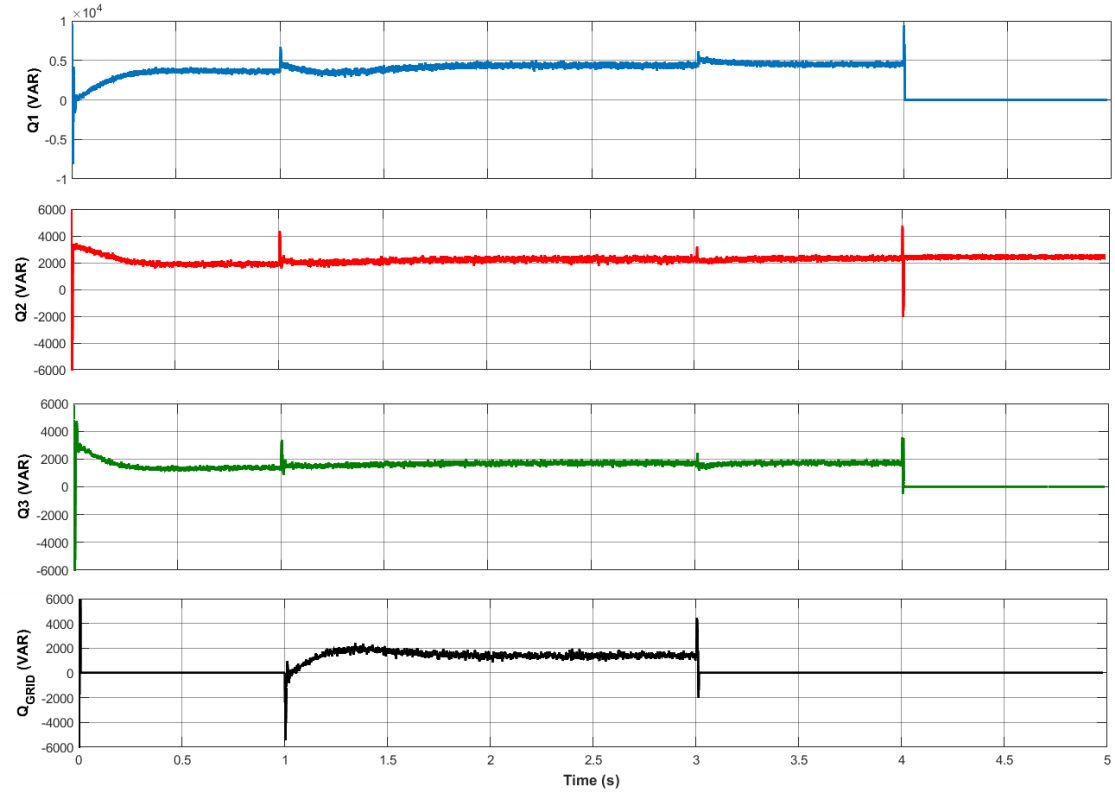


**Figure 24.** Reactive power for grid-tied scenario

## 6. CONCLUSION

The control methods of GFM inverters are discussed and reviewed. Based on literature review, it can be said that all control techniques of GFM inverters fundamentally a modified droop control because the main idea is to form frequency based on active power, and to form voltage based on reactive power. Even though they have different names, they try to mimic the synchronous generators virtually and to use an improved version of droop control. As a result of that, the weak points of the control technique are resolved to have better load sharing performance and improving the lifetime of the inverters. This enhanced control method is simulated in three different scenarios to see frequency and voltage stability and load sharing. The first case is to apply a control algorithm to observe the voltage and frequency regulation when the IBRs have equal power ratings during the off-grid. Then, the second scenario is also utilized in islanding mode where the load sharing control algorithm is executed in case of different IBRs' power ratings. In the last setup, the load sharing during the grid-tied scenario is obtained when the IBRs do not have the ability to provide enough power to the load. In all cases, the load power is changed by adding or removing the loads from the system to ensure that the frequency and voltages are recovered and do not exceed the limit based on ride-through requirements.

## DECLARATION OF ETHICAL STANDARDS

The authors of the paper submitted declare that nothing which is necessary for achieving the paper requires ethical committee and/or legal-special permissions.

## CONTRIBUTION OF THE AUTHORS

**Sahin Gullu:** Investigation, Methodology, Writing-Original draft, Simulation, Validation, Reviewing, and Editing.

**Mohammad Nilian:** Validation and Reviewing.

**Issa Batarseh:** Conceptualization, Reviewing, and Editing.

## CONFLICT OF INTEREST

There is no conflict of interest in this study.

**REFERENCES**

[1] Lasseter R H, Chen Z, Pattabiraman D. Grid-Forming Inverters: A Critical Asset for the Power Grid. IEEE Journal of Emerging and Selected Topics in Power Electronics 2020; 8(2): 925-935.

[2] Rathnayake D B, Akrami M, Phurailatpam C, Me S P, Hadavi S, Jayasinghe G, Zabihi S, Bahrani B. Grid Forming Inverter Modeling, Control, and Applications. IEEE Access 2021; 9: 114781-114807.

[3] Unruh P, Nuschke M, Strauß P, Welck F. Overview on grid-forming inverter control methods. Energies 2020;13 (10): 2589.

[4] Rezaii R, Ghosh S, Safayatullah M, Milad T S, Batarseh I. Quad-Input Single-Resonant Tank LLC Converter for PV Applications. IEEE Transactions on Industry Applications 2023; 59(3): 3438-3457.

[5] Nilian M, Rezaii R, Safayatullah M, Gullu S, Alaql F, Batarseh I. A Three-port Dual Active Bridge Resonant Based with DC/AC Output. IEEE Energy Conversion Congress and Exposition (ECCE) Nashville, TN, USA, 2023.

[6] Rezaii R, Nilian M, Ghosh S, Batarseh I, Safayatullah M. Design and Implementation of a Multiport System for Solar EV Applications. IEEE Applied Power Electronics Conference and Exposition (APEC) Orlando, FL, USA, 2023.

[7] Rezaii R, Ghosh S, Safayatullah M, Batarseh I. Design and Implementation of a Five-Port LLC Converter for PV Applications. IEEE Applied Power Electronics Conference and Exposition (APEC) Orlando, FL, USA, 2023.

[8] Rezaei M H, Akhbari M. Power decoupling capability with PR controller for Micro-Inverter applications. International Journal of Electrical Power & Energy Systems 2022; 136: 107607.

[9] Rezaei M H, Akhbari M. An active parallel power decoupling circuit with a dual loop control scheme for micro-inverters. International Journal of Electrical Power & Energy Systems 2021; 49(12): 3994-4011.

[10] Matevosyan J, Badrzadeh B, Prevost T, Quitmann E, Ramasubramanian D, Urdal H, Achilles S, MacDowell J, Huang S H, Vital V, O'Sullivan J. Grid-Forming Inverters: Are They the Key for High Renewable Penetration?. IEEE Power and Energy Magazine 2019; 17(6): 89-98.

[11] Song G, Cao B, Chang L. Review of Grid-forming Inverters in Support of Power System Operation. Chinese Journal of Electrical Engineering 2022; 8(1): 1-15.

[12] Tayyebi A, Groß D, Anta A, Kupzog F, Dörfler F. Frequency Stability of Synchronous Machines and Grid-Forming Power Converters. IEEE Journal of Emerging and Selected Topics in Power Electronics 2020; 8(2): 1004-1018.

[13] California Public Utilities Commission, Recommendations for Updating the Technical Requirements for Inverters in Distributed Energy Resources. Smart Invert. Work. Gr. Recomm. 2014. https://www.cpuc.ca.gov/-/media/cpuc-website/divisions/energy-division/documents/rule21/smart-inverter-working-group/siwgworkingdocinrecord.pdf

[14] IEEE Standard for Interconnection and Interoperability of Distributed Energy Resources with Associated Electric Power Systems Interfaces – Redline. IEEE Std 1547-2018, 2018.

[15] Gkountaras A, Dieckerhoff S, Sezi T. Evaluation of current limiting methods for grid forming inverters in medium voltage microgrids. IEEE Energy Conversion Congress and Exposition (ECCE) Montreal, QC, Canada, 2015.

[16] Du W, Chen Z, Schneider K P, Lasseter R H, Nandanoori S P, Tuffner F K. A Comparative Study of Two Widely Used Grid-Forming Droop Controls on Microgrid Small-Signal Stability. IEEE Journal of Emerging and Selected Topics in Power Electronics 2020; 8(2): 963-975.

[17] Li M, Wang Y, Xu N, Liu Y, Wang W, Wang H. A novel virtual synchronous generator control strategy based on improved swing equation emulating and power decoupling method. IEEE Energy Conversion Congress and Exposition (ECCE) Milwaukee, WI, USA, 2016.

[18] Brabandere D K, Bolsens B, Van den Keybus J, Woyte A, Driesen J, Belmans R. A Voltage and Frequency Droop Control Method for Parallel Inverters. IEEE Transactions on Power Electronics 2007; 22(4): 1107-1115.

[19] Chandorkar M C, Divan D M, Adapa R. Control of parallel connected inverters in standalone AC supply systems. IEEE Transactions on Industry Applications 1993; 29(1): 136-143.

[20] Karimi-Davijani H, Ojo O. Dynamic operation and control of a multi-DG unit standalone Microgrid. ISGT Anaheim, CA, USA, 2011.

[21] Singhal A, Vu T L, Du W. Consensus Control for Coordinating Grid-Forming and Grid-Following Inverters in Microgrids. IEEE Transactions on Smart Grid 2022; 13(5): 4123-4133.

[22] Nasirian V, Shafiee Q, Guerrero J M, Lewis F L, Davoudi A. Droop-Free Distributed Control for AC Microgrids. IEEE Transactions on Power Electronics 2016; 31(2): 1600-1617.

[23] Du W, Lasseter R H, Khalsa A S. Survivability of Autonomous Microgrid During Overload Events. IEEE Transactions on Smart Grid 2019; 10(4): 3515-3524.